Norsk Geografisk Tidsskrift – Norwegian Journal of Geography Vol. 56, 257–264. Oslo. ISSN 0029-1951

Post-glacial rock weathering processes on a roche moutonnée in the Riksgränsen area (68°N), northern Norway

JOHN C. DIXON, COLIN E. THORN, ROBERT G. DARMODY & SEAN W. CAMPBELL

Dixon, J. C., Thorn, C. E., Darmody, R. G. & Campbell, S. W. 2002. Post-glacial rock weathering processes on a roche moutonnée in the Riksgränsen area (68°N), northern Norway. *Norsk Geografisk Tidsskrift–Norwegian Journal of Geography* Vol. 56, 257–264. Oslo. ISSN 0029-1951.

Weathering processes responsible for landscape denudation in Arctic environments are poorly understood. Traditionally, gelifraction has been widely invoked as the dominant weathering process, but empirical support for this is frequently lacking. In Norwegian Lapland, post-glacial weathering has been recently attributed to predominantly biophysical processes, based on field measurements of landscape lowering undertaken by André (1995). The study reported here examined bedrock samples from one of André's sites for mineralogical and chemical transformations since post-glacial exposure. Backscatter scanning electron microscopy reveals extensive mineral grain dissolution and accompanying development of rock porosity. Wavelength dispersive spectroscopy shows these mineral alterations to be the result of the loss of major chemical constituents including Ca, Mg, K, Si, and Al. Chemical weathering is clearly a component of post-glacial landscape denudation in Norwegian Lapland, in addition to the important role of biophysical processes identified by André (1995). Cosmogenic dating of the sampled bedrock surface confirms that much of this weathering has occurred in the last 10,000 years.

Keywords: *chemical weathering, landscape evolution, Lapland.*

John C. Dixon, Department of Geosciences, University of Arkansas, Fayetteville, AR 72701, USA. E-mail: jcdixon@uark.edu; Colin E. Thorn, Department of Geography, University of Illinois, Urbana, IL, 61801, USA; Robert G. Darmody, Department of Natural Resources and Environmental Sciences, University of Illinois, Urbana, IL, 61801, USA; Sean W. Campbell, Department of Geography, University of Kentucky, Lexington, KY 40506, USA

Introduction

The nature and rate of weathering processes effecting post-glacial landform and landscape change in Arctic environments is poorly understood. In 1995 André, working in the Riksgränsen area of northern Norway and the adjacent Låktatjåkka and Vassijaure areas of Sweden, examined post-glacial microweathering using the methods of Dahl (1967). Her estimates were based on measurements of depth of lowering below a datum of glacially-polished surfaces, weathering pit geometry, and joint width. From these measurements she suggested that weathering rates were extremely low, finding that surface lowering was in the order of 0.2–1.0 mm Ka^{-1}, pit depth growth was 2–3.5 cm since deglaciation, and joint widening was c. 2 cm over the same time period. She suggested that the effects of microgelivation were weak, and that most of the observed and measured microweathering was primarily effected by a variety of biological processes. These processes appeared to be largely physical in nature. They include the forces generated by changes in lichen thalli due to wetting and drying as well as by the penetration of lichen rhizine and hypha along biotite cleavage planes and mineral grain boundaries, though biochemical processes were also envisioned to occur. The purpose of the research presented here was to examine chemical weathering processes operating on the bedrock at one of André's sites, a task beyond the capability of her field techniques, but feasible with scanning electron microscopy (SEM) and microprobe techniques.

Determination of weathering rates in this northern location rests strongly upon an ability to determine landscape age. In many instances this is the time since emergence from beneath the Fennoscandian ice sheet. However, there is increasing evidence in northern Scandinavia for the occurrence of cold-based ice that was largely protective, rather than erosive (Kleman 1992). Therefore, much care must be taken in assessing the time during which observed weathering has accumulated. André based her weathering rate calculations on a mean deglaciation age of 10,000 BP. She arrived at this age largely by averaging the available ^{14}C ages for the region (Sonesson 1974, Sollid 1989, Kleman 1992). Since the time of these published dates new assessments have been made which generally bring the age of deglaciation forward (Berglund et al. 1996). None of these dates, however, have been drawn from the roches moutonnées that formed the core of the surfaces studied by André. We dated the surface of a single roche moutonnée within André's Bj2 field investigation plot using ^{36}Cl dating methods to obtain a known age of deglaciation at the site, and tied our weathering observations to it. We presume the ice in the bottom of a major glaciated valley to have been erosive.

Research area

The study area is located in northern Norway, immediately west of the international border with Sweden, at approximately 68°25′N and 18°05′W and at an elevation of c. 500 m a.s.l. (Fig. 1). The glaciated landscape is eroded in Precambrian biotite granites of the Rombak window, and displays a typical 'knob and basin' topography with lake-filled rock basins and intervening roches moutonnées. The Rombak granite, occurring in the core of the Scandes Mountains, is a gray, coarse-grained biotite granite containing large phenocrysts of microcline. Both grain size and biotite content are locally variable. The most acid varieties are represented by

Taylor & Francis
Taylor & Francis Group

© 2002 Taylor & Francis

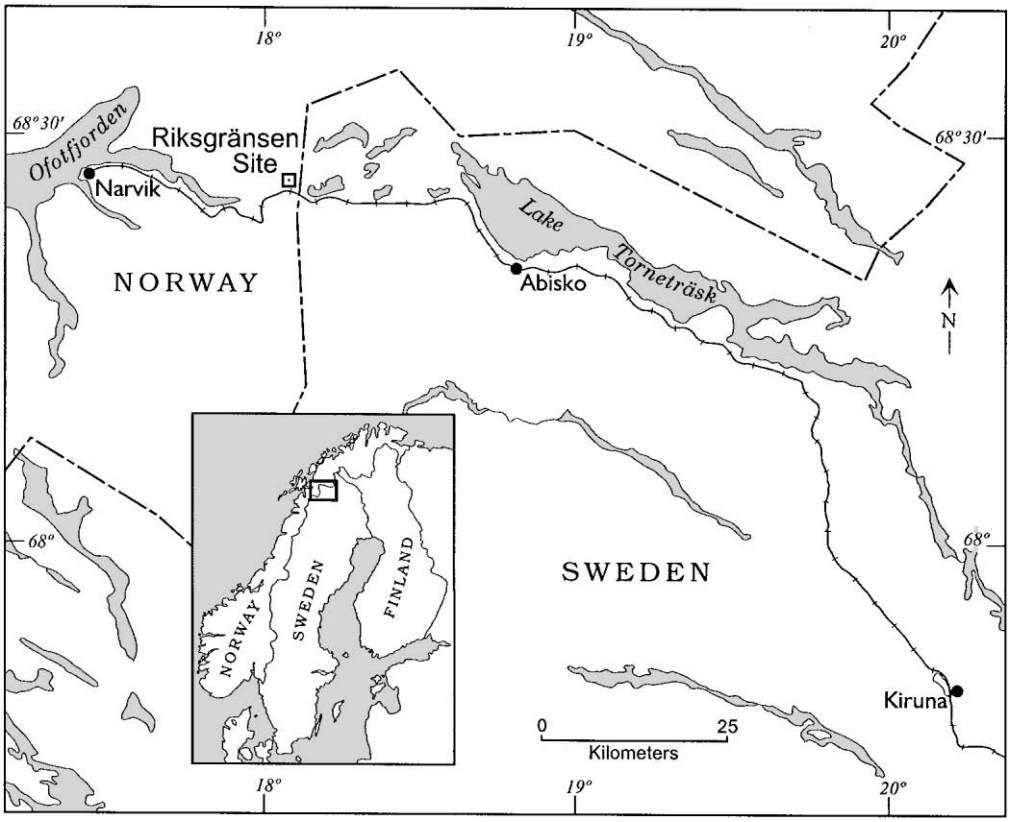

Fig. 1. Location of Riksgränsen study site.

fine-grained banded migmatite and by coarse-grained granite or syenite, which contain in excess of 60% alkali feldspar. Biotite-rich xenoliths are abundant, occurring together with veins of aplite, quartz and pegmatite.

The study site lies in a transition zone between the maritime climate of coastal Norway c. 70 km to the west and the drier, more continental climate to the east. A nearby weather station at Katterjåkk to the south-east records mean annual precipitation of 940 mm, with half of it falling as snow, and a mean annual temperature range of −11°C in January to 10°C in July. The study area is located altitudinally immediately above the subalpine birch forest dominated by *Betula pubescens* ssp. *tortuosa*. The roches moutonnées support an extensive (75%) cover of crustose and foliose lichens (including *Rhizocarpon* sp., *Haematomma ventosum, Lecidea lithophila, Parmelia centrifuga*, and several species of *Umbilicaria*), as well as moss carpets on their lower slopes. In the swampy areas which surround the lakes that occupy nearby depressions, dwarf willow and various species of arctic cotton grass dominate (André 1995).

Methods

A single roche moutonnée at André's (1995) Bj2 site (Fig. 2A) was sampled. Rock hammers and chisels were used to collect approximately one kilogram of rock from the crest of the outcrop for cosmogenic dating purposes. The crest site was selected for the dating sample in order to minimize shading of cosmogenic rays. The same tools were used to sample the bottom of a weathering pit (Rk2), and an inside face of a joint (Rk3) on a glacially-polished section of the roche moutonnée, while the third sample (Rk1) came from the crag or stoss side of the roche moutonnée (Fig. 2B). Two samples were taken from each of Rk microsites, they are designated a and b suffixes in the text.

Small, multi-mineralic rock fragments were placed in 2.5 cm diameter stainless steel circular molds and filled with epoxy. Upon hardening of the resin, the epoxy disks were removed from the molds and the upper surfaces polished with progressively finer aluminum powder grits down to 0.3 μm size. Polished samples were then thoroughly washed with distilled water, dried, and mounted on a sample holder, carbon-coated to reduce electron scattering, and loaded into a JOEL JXA-8600 Superprobe operated at 15 keV. Samples were oriented such that the imaged area was a cross-section of rock extending from the outer surface into the interior core.

Images of rock fragments were captured and stored as digital files using backscatter electron microscopy (BSE). The images were formed by backscattered electrons, which show variations in chemical composition based on average atomic number. Lower atomic number elements appear dark,

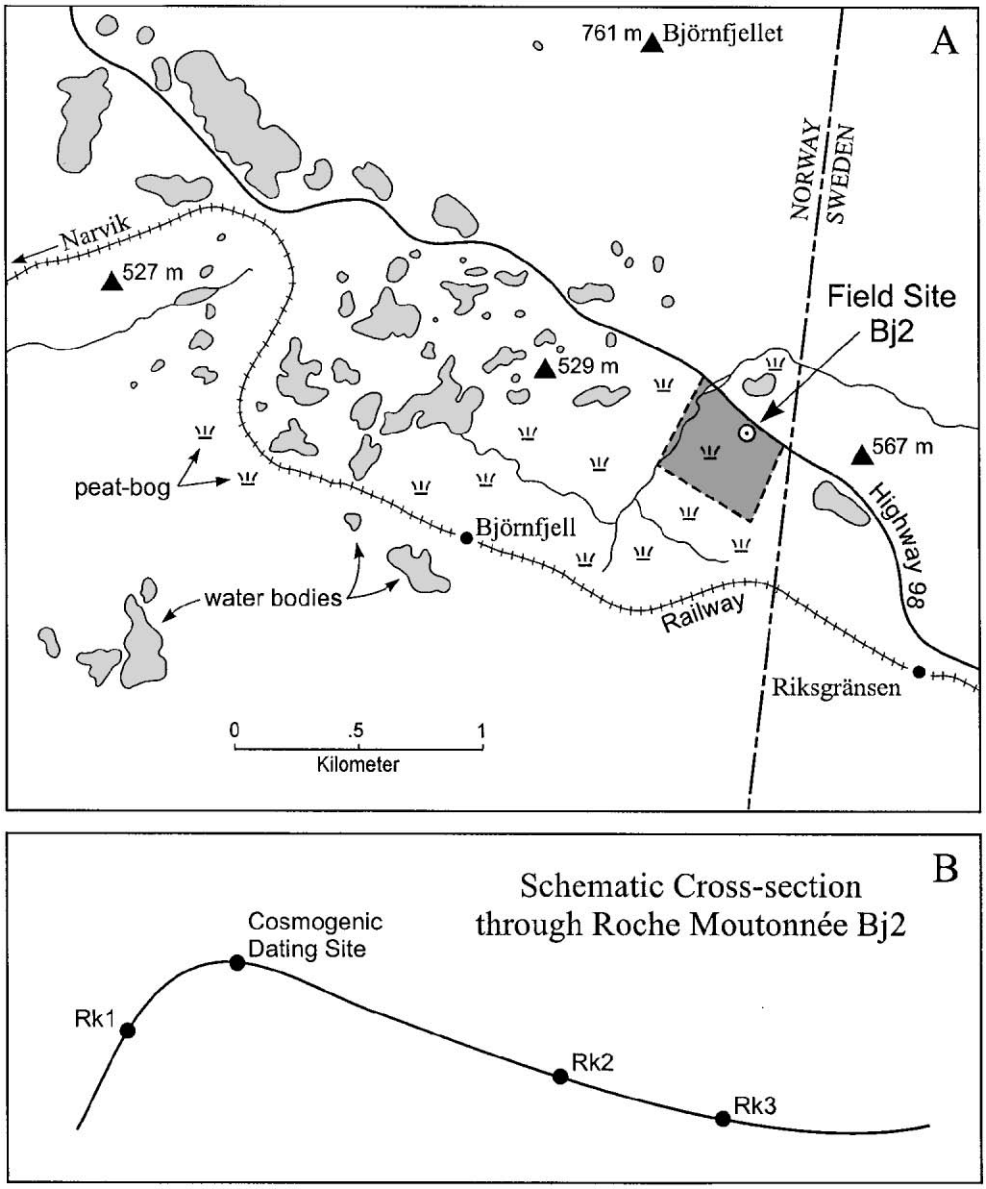

Fig. 2. A: Location of sampled roche moutonnée simplified from André (1995, Figure 7.2). The shaded area is André's original Bj2 research plot; the bull's eye symbol in the figure designates our site. B: schematic profile through roche moutonnée showing individual sampling points for cosmogenic dating and analysis. Two samples were taken from each microsite at Rk1, Rk2, and Rk3, and in the text the two individual samples are identified by addition of the suffixes a and b.

while higher number elements appear bright (Krinsley & Manley 1989).

Chemical analyses of rock samples were obtained using the wavelength dispersive spectroscopy mode on the JOEL JXA-8600 Superprobe. Analyses were made along transects extending from the outer edge to the inner portion of the sample, with analysis points equi-spaced along the transect. Peak count times of 7 minutes were employed for each analysis using a diffuse beam width of 80 μm. This diffuse beam width and short count time assures against the 'vaporization' of light elements. Chemical analyses typically total less than 100% due to sample porosity, and the presence of water and organics (Dorn 1995). Chemical analyses of selected mineral grains were recalculated as ratios of mobile to immobile elements (Birkeland 1999, 66) to assess the amount of weathering that had occurred. Two minerals for which comparisons of the chemistry of pitted versus unpitted surfaces could be made were selected. For the biotite grain, mobile elements were compared to titanium (Ti) as this element is generally regarded as being especially immobile in the weathering environment. For the plagioclase, mobile elements were compared to aluminum (Al) as this mineral contains minimal Ti and aluminum is also generally regarded as a relatively immobile element (Birkeland 1999).

Cosmogenic dating using ^{36}Cl was conducted at the PRIME laboratory at Purdue University in Indiana using

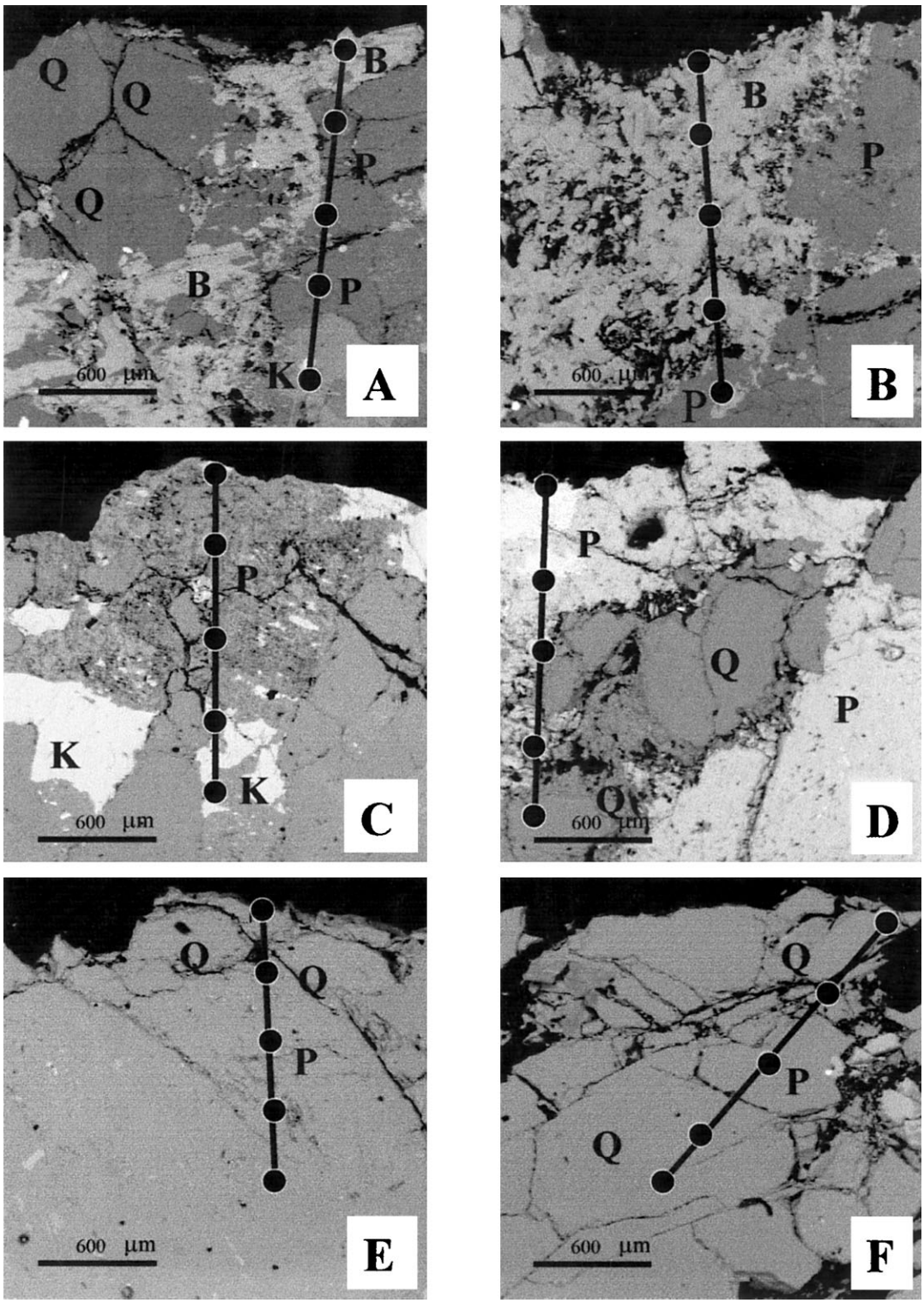

Fig. 3. Backscatter scanning electron micrographs of rock samples from roche moutonnée. Black lines represent analytical transects and dots show locations of chemical analyses presented in Table 2. Analyses are from top to bottom of transect line. Dissolution of mineral grains and grain boundaries is indicated by black areas. A. Sample Rk1a. Cleavage controlled dissolution of biotite (B), and mineral grain dissolution of Na-plagioclase (P) and K-feldspar (K). Note also strongly developed grain boundary dissolution of feldspar and quartz (Q). B. Sample Rk1b. Extensively dissolved biotite grain (B) shown by the dark areas. C. Sample Rk2a. Extensively dissolved plagioclase feldspar grain (P). Note orientation of dissolution voids in the vertical direction. Potassium feldspar grains (K) appear to be less extensively pitted. D. Sample Rk2b. Extensively pitted plagioclase feldspar grains (P) showing some evidence of preferred orientation of pitting. Quartz (Q) appears to be substantially less pitted, with most dissolution concentrated around grain edges. Bright mineral grains at points 1 and 2 are Ti-rich amphibole (perhaps astrophyllite). E. Sample Rk3a. Pitted plagioclase feldspar grain (P) with grain boundary dissolution. F. Sample Rk3b. Quartz grains showing little surface pitting, but with extensive grain boundary dissolution.

the methods of Phillips et al. (1986). Chemical analyses for age determination calculations were conducted at the XRAL laboratories in Canada. Age determinations were made using CHLOE software from the New Mexico Department of Mines (Phillips & Plummer 1996).

Rock porosity was calculated following the methods of Dorn (1995). These methods involve obtaining backscatter digital images of weathered rock samples for analysis in image processing software. Mounting epoxy and surface organics are 'cut out' of the image. Histograms of the remaining image data reveal peaks of gray scale values representing different minerals and porosity. The histograms are used to determine the range of gray values between 0 (white) and 255 (black), as well as the mean value. All gray values above the fourth standard deviation from the mean are assumed to represent pore space. A threshold image is created which shows only the pixels higher than this value. The number of pixels calculated as pore space was counted using a histogram. This number was subtracted from the total number of pixels in the image to determine the percentage of pore space in the entire image.

Results

Cosmogenic ^{36}Cl dating of the roche moutonnée Bj2 reveals an age of $10{,}300 \pm 1{,}288$ years, essentially affirming André's 10,000 year estimate for deglaciation of the study area based on existing radiocarbon ages. In the BSE analysis, the assumption is made that at the time of glaciation, all weathered debris is removed by the passage of glacial ice and that the newly exposed post-glacial surface is pristine, unaltered bedrock. Consequently, all mineralogical modifications that are observed are assumed to be post-glacial in origin. This latter assumption is supported to a large degree by the observations from Kärkevagge, c. 10 km to the east, that beneath weathering rinds on rock debris the bedrock core is fundamentally unaffected by chemical weathering as indicated by rock porosities near zero (Dixon et al. 2002).

Micromorphology

Examination of the BSE micrographs of bedrock samples from three sites on the roche moutonnée, as well as chemical analysis of mineral grains, reveals evidence of discernible and measurable chemical weathering since deglaciation (Fig. 3). The impact of chemical alteration is seen in the dominant rock-forming minerals of biotite, Na-rich plagioclase feldspar, K-rich feldspar, and quartz. The greatest amount of alteration is concentrated in mineral grains at/or adjacent to the bedrock surface.

Biotite: biotite weathering involves primarily mineral grain dissolution, with little evidence of oxidation. Two forms of dissolution are apparent in the micrographs. In Fig. 3A, the central part of the image, immediately to the left of the scan line, is dominated by biotite (B). The biotite grain displays evidence of dissolution as shown by dark void spaces. The smaller, linear, void spaces have a tendency to be oriented parallel to cleavage. This structural control on dissolution is not as apparent in the biotite grain displayed in Fig. 3B, where the biotite displays the development of larger voids in the grain center, with little evidence of distinctive alignment.

Table 1. Weathered rock porosities (%) from surface of roche moutonnée.

Sample #	Porosity (%)
Rk1a	11.9
Rk1b	7.5
Rk2a	3.1
Rk2b	15.0
Rk3a	6.2
Rk3b	8.5
Mean	8.7

Feldspars: the bedrock is overwhelmingly dominated by Na-rich plagioclase feldspar, but also contains minor amounts of K-rich feldspars. The Na-rich plagioclase feldspar (P), displays extensive dissolution (Figs. 3C and 3E). This dissolution is reflected in the extensive development of voids in grain interiors, indicated by the dark areas. In addition, there is evidence of grain boundary dissolution as reflected in the dark linear bands surrounding and crossing the grain boundaries. In all cases, the Na feldspars display greater weathering than the K-feldspars (K), as indicated by the apparent higher frequency of dissolution voids (Figs. 3A and 3C). Apparent alignment of the dissolution voids, appearing as dark linear bands within feldspar grains (P) in Figs. 3C and 3D, suggests that the dissolution of feldspars is structurally controlled.

Quartz: while quartz is normally regarded as being a relatively resistant mineral with respect to chemical weathering, there is extensive evidence of its dissolution in the samples examined in this study. Dissolution, however, appears to be largely confined to grain boundaries, where solutional embayments are visible along grain edges. Despite overall limited evidence of grain interior dissolution, some dissolution voids are visible. These voids are seen as essentially round black holes on quartz (Q) grains in Figs. 3D and 3F.

Rock porosity: porosity is a measure of geochemical mass loss and corresponds to the amount of geochemical dissolution that has occurred in the sample (Table 1). Porosity ranges from 3.1% in sample Rk2a where grain surface and grain boundary dissolution are clearly limited in extent (Fig. 3C), to 15% in sample Rk3b where grain boundary dissolution of the quartz is dominant (Fig. 3D). The average porosity of the 6 analyses conducted in this study is almost 9%. In all of the images it is apparent that there is enhanced porosity, especially grain boundary porosity, in the vicinity of the outer edge of the sample.

Geochemistry

Geochemical data from the six samples examined with the

Table 2. Major element geochemistry from wavelength dispersive spectroscopy along scan lines shown in Fig. 3.

Point	Na %	Mg %	Al %	Si %	P %	S %	K %	Ca%	Ti %	Cr %	Mn %	Fe %	Total %
Rk1a													
1	0.121	6	16.098	32.547	0.013	0.016	7.159	0.096	1.687	0.017	0.299	24.996	89.049
2	10.962	0.056	19.36	63.333	BDL	BDL	0.548	0.166	BDL	BDL	0.009	0.307	94.741
3	5.31	3.281	18.239	48.78	0.062	0.039	2.844	0.287	0.802	BDL	0.161	12.865	92.67
4	12.929	0.025	19.993	66.304	0.02	0.011	0.255	0.384	BDL	BDL	0.009	0.092	100.02
5	3.501	0.007	18.944	60.455	0.008	0.011	9.742	0.757	0.007	BDL	0.031	0.026	93.479
Rk1b													
1	0.082	6.32	16.453	32.217	BDL	0.008	7.729	0.027	1.59	0.097	0.371	24.279	89.173
2	0.012	5.667	15.543	30.697	0.043	0.018	7.426	0.086	1.449	0.121	0.413	25.031	86.506
3	0.101	5.717	13.929	27.711	0.128	0.028	5.634	1.13	2.683	0.1	0.241	21.606	79.008
4	0.036	5.834	16.339	30.406	0.043	0.007	5.945	0.078	1.496	0.086	0.173	23.444	83.887
5	12.074	BDL	19.608	62.85	0.013	BDL	0.188	0.185	BDL	0.072	BDL	0.15	95.14
Rk2a													
1	0.459	BDL	17.689	62.233	BDL	BDL	15.187	0.032	BDL	0.197	0.023	0.012	95.832
2	11.123	BDL	21.793	64.562	0.001	BDL	0.077	2.997	BDL	0.188	BDL	0.12	100.881
3	12.011	BDL	19.241	57.088	BDL	BDL	0.019	0.769	0.014	0.147	BDL	0.103	89.392
4	4.438	BDL	22.996	55.458	BDL	0.049	7.197	0.221	BDL	0.178	0.001	0.029	90.567
5	11.613	BDL	20.071	66.069	BDL	BDL	0.123	0.683	BDL	0.19	0.01	0.036	98.795
Rk2b													
1	0.057	0.729	5.423	59.858	0.099	BDL	0.196	4.481	10.299	0.044	0.161	10.783	92.13
2	0.026	0.111	3.18	52.175	0.009	BDL	0.028	7.394	18.991	0.078	0.043	4.376	86.411
3	5.6	0.015	16.729	54.837	0.033	0.111	0.058	0.631	0.633	0.017	0.04	2.344	81.048
4	5.081	0.013	11.007	39.655	0.003	0.039	0.027	1.789	0.001	0.088	BDL	0.045	57.748
5	BDL	0.016	0.333	97.343	0.073	BDL	0.013	0.007	0.001	BDL	0.061	0.003	97.849
Rk3a													
1	BDL	BDL	0.012	96.708	BDL	0.024	0.008	0.007	BDL	BDL	0.009	0.016	96.772
2	0.019	BDL	0.698	97.493	0.026	0.011	0.02	BDL	BDL	0.062	BDL	BDL	98.329
3	5.054	0.006	13.449	69.25	0.078	0.006	0.045	0.771	0.004	0.041	0.009	0.081	88.794
4	5.075	0.008	11.209	79.455	BDL	0.008	0.031	1.585	0.021	0.043	0.07	0.013	97.518
5	4.577	0.009	10.525	76.504	0.008	0.037	0.032	1.296	0.003	0.014	0.031	0.137	93.173
Rk3b													
1	0.006	0.002	0.036	93.217	0.009	0.025	0.007	0.005	BDL	0.007	0.074	0.007	93.395
2	0.002	0.08	0.891	3.031	0.01	0.287	0.014	0.096	0.001	0.008	0.035	0.086	4.451
3	0.04	0.015	14.633	64.796	0.029	0.039	0.053	0.132	BDL	0.014	0.07	0.063	79.814
4	0.003	0.006	0.144	95.904	0.003	0.029	BDL	0.023	0.007	BDL	0.018	0.038	96.175
5	BDL	0.003	0.191	97.434	0.031	0.011	0.002	0.017	0.01	0.041	0.066	0.002	97.808

BDL = Below detectable limits.

electron microprobe are presented in Table 2. The single most significant point from the geochemical data is that chemical totals, with one exception, are less than 100%. This observation is a reflection of the fact that chemical mass is being lost as a result of mineral grain dissolution reflected in the rock porosity reported in the previous section. The presence of dissolution voids, coupled with low geochemical totals, reveals the pattern of geochemical loss associated with bedrock weathering. The biotite grain represented by sample Rk1b in Table 2 and Fig. 3B displays lower abundances of Si, K, Mg, and Al in pitted compared to non-pitted grains. Comparison of ratios of mobile to immobile elements confirms that these lower abundances represent real chemical loss. The elemental ratios of K, Mg, Si, and Al (mobile) to Ti (immobile) all showed marked decreases from analysis points 1, 2 and 4 to point 3 (Table 3). As biotite weathering commonly involves loss of Al (Borchardt 1977) this chemical constituent is regarded as mobile in the case of biotite. The plagioclase grain of sample Rk2a (Table 2 and Fig. 3C) displays evidence of a loss of Ca, Na, and Si as seen in the comparison of point 4 to points 2, 3, and 5. Elemental ratios of these mobile elements to immobile (Al) all show a decrease in point 4 values compared to those of points 2, 3, and 5 (Table 4). Quartz dissolution is extremely limited, Si

Table 3. Ratios of mobile to immobile elements from pitted (point 3) and non-pitted (points 1, 2, 4) biotite grain in Fig. 3B.

Sample	K:Ti	Mg:Ti	Si:Ti	Al:Ti
Rk1b				
Point 1	4.86	3.97	20.26	10.35
Point 2	5.13	3.91	21.18	10.73
Point 3	2.10	2.13	10.32	5.19
Point 4	3.98	3.90	23.32	10.92

Table 4. Ratios of mobile to immobile elements from pitted (point 4) to non-pitted (points 2, 3, 5) plagioclase feldspar grain in Fig. 3C.

Sample	Ca:Al	Na:Al	Si:Al
Rk2a			
Point 2	0.14	0.50	2.96
Point 3	0.03	0.60	2.97
Point 4	0.01	0.19	2.60
Point 5	0.03	0.60	3.29

totals essentially correspond to elemental totals, with greatest loss apparently associated with grain boundary dissolution. This is reflected in the extremely low Si value for sample Rk3b point 2, which is associated with a major void.

Discussion

André (1995) clearly established that since post-glacial exposure, at an estimated 10,000 years ago, roches moutonnées in Norwegian Lapland have experienced limited, but measurable, weathering. Our ^{36}Cl age of $10{,}300 \pm 1{,}300$ compares well with André's age estimate from multiple ^{14}C ages. In the absence of credible evidence for microgelifraction as the dominant weathering mechanism (Swantesson 1985), André attributed the observed weathering largely to the growth of lichen thalli which frequently contained both biotite and feldspar flakes and fragments within decaying thalli centers. Incorporation of mineral fragments is suggested to be largely the result of rhizine and hyphal penetration along cleavage planes and grain boundaries, which presumably weakens grain boundary cohesion and eventually leads to rock disintegration. Production of enlarged pathways subsequently further facilitates colonization by additional lichens (André 1995). In addition, she speculates that expansion and contraction of algal mucilage associated with wetting and drying of bedrock surfaces may also induce mineral flaking. While the growth of moss cushions and their subsequent migration across bedrock surface are also presented as possible weathering mechanisms, no evidence for a measurable impact was observed. It is important to note that all three of these weathering mechanisms are envisaged to be fundamentally biophysical in nature, with no direct evidence of chemical influences reported. However, a particular susceptibility of biotite-rich rocks is indicated, but this is presumably due to the fissile nature, and hence ready susceptibility, of biotite to mechanical disruption.

This present study demonstrates that the surface lowering, weathering pit development, and fracture expansion reported and measured by André (1995) is also in part attributable to chemical weathering of biotite, feldspar, and quartz grains in the bedrock. We have demonstrated through BSE microscopy and wavelength dispersive spectroscopy that all of these minerals are affected by dissolution and consequently experience loss of major chemical constituents including Na, Ca, Si, Al, and K. Mineral grain dissolution has resulted in the development of an average near-surface rock porosity of c. 9% in approximately 10,000 years. The development of mineral grain porosity as an important and widespread consequence of chemical weathering has been widely recognized (Worden et al. 1990 Anbeek et al. 1994). This interpretation is based on the assumption that with the removal of the ice the new bedrock surface was truly completely unweathered. While primary porosity certainly occurs in igneous rocks, the apparent preferential development of this phenomena at sample surfaces suggests that the observed porosity is largely due to the effects of chemical weathering since post-glacial ice removal, when the weathering system clock was essentially 're-set' (Dorn 1995).

While the initiation of grain boundary porosity might be viewed as resulting from micro-gelifraction, we believe this to be of little importance in the study area. Recent studies of boulder-top temperature in Kärkevagge immediately to the east (Thorn et al. 2002) have shown that the present prevailing thermal regimes are not conducive to strong freeze-thaw weathering. While beyond the immediate scope of this study, it is possible that the grain boundary pores do represent subsequent chemical exploitation of biologically, or mechanically, induced microfractures (for a discussion see Hall et al. in press).

The chemical alteration processes described above can all be attributed to normal inorganic dissolution processes involving reactions of metal cations with hydrogen dissolved in water and the subsequent production of dislodged metal cations from the mineral structure. However, as noted at the beginning of this paper, the roches moutonnées in the study area carry an extensive covering of lichens, up to 75%, so it is also possible that the observed chemical weathering is enhanced by reactions with organic acids. The role of lichens in effecting and enhancing chemical weathering has been widely debated, with many workers arguing for a significant role in weathering as a result of the production of respiratory CO_2, excretion of oxalic acids, and the production of a variety of biochemical compounds with complexing ability (Syers & Iskander 1973, Williams & Rudolf 1974, Berthelin 1983). However, in a recent review of biogeochemical weathering processes, Barker et al. (1997) argue that it is possible that overall, lichens do not play a significant role in chemical weathering because many of the organic acids produced by these organisms are, in fact, stored in the upper parts of the lichen thalus, away from the rock interface where chemical weathering occurs. Nevertheless, this statement should not be generalized to all lichen species. Recent studies from Iceland (e.g. Etienne 2001) clearly demonstrate the biochemical effectiveness of lichens such as *Lecanora rupicola* (L) Zahlbr. in cold environments.

Conclusions

From the above analysis, it is apparent that chemical weathering of post-glacially exposed roches moutonnées in Arctic Norway is active. The dominant chemical weathering process is apparently dissolution of aluminosilicate minerals and quartz, which in the span of 10,000 years has resulted in the loss of mobile chemical constituents and associated development of a porous texture of up to as much as 15%, with an average of approximately 9%. It is therefore apparent that in addition to the biophysical processes outlined by André (1995) in effecting post-glacial landscape lowering, geochemical, and potentially biogeochemical processes are also making substantial contributions to landscape denudation in the Arctic environment of Norwegian Lapland. The next step in this work is to use secondary scanning electron microscopy to establish if the grain boundary voids are occupied by lichen rhizine or are primarily solutional, thereby formally linking André's work to ours. This was not undertaken in the present study as the focus was on identifying the nature of chemical processes operating on

mineral grains. In the absence of direct investigation, the overall physical integrity of the roches moutonnées does not suggest that freeze-thaw weathering is substantial, or should be invoked in preference to research clearly establishing the presence of biophysical and chemical processes.

Acknowledgements.–Fieldwork and cosmogenic dating was supported by grants BCS-9818917 and BCS-9818667 from the National Science Foundation. Backscatter electron microscopy and electron microprobe analyses of rock samples were conducted at Arizona State University (ASU) where the assistance of Mr Jim Clark was greatly appreciated. The JOEL superprobe laboratory at ASU is supported by NSF grant 89-00403. The Abisko field station provided logistical support throughout the project. We offer thanks to all of the above organizations. We also offer our thanks to Professor Marie-Françoise André for her active and helpful cooperation in our pursuit of this project.

Manuscript submitted 1 February 2002; accepted 15 June 2002

References

Anbeek, C. V. B., Breemen, N., Meijer, E. & Van Der Plas, L. 1994. The dissolution of naturally weathered feldspar and quartz. *Geochimica Cosmochimica Acta* 58, 4601–4610.

André, M. F. 1995. Post-glacial microweathering of granite roches moutonnées in northern Scandinavia (Riksgränsen area 68°N). Slaymaker, O. (ed.) *Steepland Geomorphology*, 103–127. John Wiley and Sons, London.

Barker, W. W., Welch, S. A. & Banfield, J. F. 1997. Biogeochemical weathering of silicate minerals. Banfield, J. F. & Nealson, K. H. (eds.) Geomicrobiology: interactions between microbes and minerals. *Reviews in Mineralogy* 35, 391–428.

Berglund, B. E., Barnekow, L., Hammarlund, D., Sandgren, P. & Snowball, I. F. 1996. Holocene forest dynamics and climate changes in the Abisko area, northern Sweden – the Sonesson model of vegetation history, reconsidered and confirmed. *Ecological Bulletins* 45, 15–30.

Berthelin, J. 1983. Microbial weathering processes. Krumbein, W. E. (ed.) *Microbial Geochemistry*, 223–264. Blackwell Scientific Publishers, Oxford.

Birkeland, P. 1999. *Weathering and Soils*. Oxford University Press, New York.

Borchardt, G. A. 1977. Montmorillonite and other smectite minerals. Dixon, J. B. & Weed, S. B. (eds.) *Minerals in Soil Environments*, 393–330. Soil Science Society of America, Madison.

Dahl, R. 1967. Post-glacial micro-weathering of bedrock surfaces in the Narvik district of Norway. *Geografiska Annaler* 49A, 155–166.

Dixon, J. C., Thorn, C. E., Darmody, R. G. & Campbell, S. W. 2002. Weathering rinds and rock coatings from an Arctic alpine environment, northern Scandinavia. *Geological Society of America Bulletin* 114, 226–238.

Dorn, R. I. 1995. Digital processing of backscatter electron imagery: a microscopic approach to quantifying chemical weathering. *Geological Society of America Bulletin* 107, 725–741.

Etienne, S. 2001. *Les processus de météorisation des surfaces volcaniques en Islande – approche épistémologique de la géomorphologie des milieux froids*. PhD thesis, University of Paris-Sorbonne. 477 pp.

Hall, K., Thorn, E., Matsuoka, N. & Prick, A. Weathering. *Progress in Physical Geography*. In press.

Kleman, J. 1992. The palimpsest glacial landscape in northernwestern Sweden. *Geografiska Annaler* 74A, 305–325.

Krinsley, D. H. & Manley, C. R. 1989. Backscattered electron microscopy as an advanced technique in petrography. *Journal of Geological Education* 37, 202–209.

Phillips, F. M. & Plummer, M. A. 1996. CHLOE: a program for interpreting in-situ cosmogenic nucleid data for surface exposure dating and erosion studies. *Radiocarbon* 38, 98–99.

Phillips, F. M., Leavy, B. D., Jannik, N. O., Elmore, D. & Kubik, P. K. 1986. The accumulation of ^{36}Cl in rocks: a method for surface exposure dating. *Science* 231, 41.

Sollid, J. L. 1989. *Northern Norway, Finland, Sweden: excursion guide. Fifth International Permafrost Conference, August 2–5, 1988*. Naturgeografisk serie, 12. Meddelelser fra Geografisk Institut, Universitetet i Oslo. 105 pp.

Sonneson, M. 1974. Late Quaternary forest development of the Torneträsk area, North Sweden. 2. Pollen analytical evidence. *Oikos* 25, 288–307.

Swantesson, J. 1985. Preliminary results from experimental weathering studies. *Fennia* 163, 303–307.

Syers, J. K. & Iskandar, I. K. 1973. Pedogenic significance of lichens. Ahmadjian, V. & Hale, M. E. (eds.) *The Lichens*, 225–248. Academic Press, New York.

Thorn, C. E., Darmody, R. G., Allen, C. E. & Dixon, J. C. 2002. Near-surface ground temperature regime variability in selected microenvironments, Kärkevagge, Swedish Lapland. *Geografiska Annaler* 84A, 289–300.

Williams, M. E. & Rudolph, E. D. 1974. The role of lichens and associated fungi in the chemical weathering of rock. *Mycologia* 66, 648–660.

Worden, R. H., Walker, F. D., Parsons, I. & Brown, W. L. 1990. Development of microporosity, diffusion channels and deuteric coarsening in perthitic alkali feldspars. *Contributions in Mineralogy and Petrology* 104, 507–515.